UNIVERSITY OF OKLAHOMA

GRADUATE COLLEGE

ADSORPTION OF BIOMASS TORREFACTION VAPORS ON ACTIVATED CARBON

A THESIS

SUBMITTED TO THE GRADUATE FACULTY

in partial fulfillment of the requirements for the

Degree of

MASTER OF SCIENCE

By

DAVID J BJERKAAS
Norman, Oklahoma
2017

ADSORPTION OF BIOMASS TORREFACTION VAPORS ON ACTIVATED CARBON

A THESIS APPROVED FOR THE
SCHOOL OF CHEMICAL, BIOLOGICAL AND MATERIALS ENGINEERING

BY

_____
Dr. Lance Lobban, Chair

_____
Dr. Richard Mallinson

_____
Dr. Daniel Resasco

© Copyright by DAVID J BJERKAAS 2017
All Rights Reserved.

Acknowledgements

I would like to thank all the members of the OU Biofuels research group for providing me with their advice and friendship as I conducted my research.

I would like to thank all the professors in our department who taught me, guided me, and inspired me throughout my time at the University of Oklahoma.

I would like to thank my family for their undying love and support.

Table of Contents

List of Figures

Abstract

Energy is a growing need for the modern economy; however, global reliance on nonrenewable resources is problematic. The United States transportation infrastructure in particular was built around the combustion of petroleum based liquid fuels providing the needed energy. Biofuels could be a potential replacement.

A promising method of producing biofuels is a staged thermal fractionation of solid biomass, also known as the torrefaction process. Three biopolymers make up lignocellulosic biomass: cellulose, hemicellulose, and lignin. Each of these biopolymers decompose within different temperature ranges to give different product distributions. Given that these temperature ranges only partially overlap, choosing reaction conditions going from a less severe stage 1 to a most severe stage 3 can allow for more homogenous product streams with respect to functionality. This eases the subsequent upgrading process.

The torrefaction product from stage 1 is not entirely composed of hemicellulose products; phenolic compounds are present which deactivate catalysts used to upgrade the majority of the stage 1 product streams. In order to ensure acceptable catalyst life, these compounds must be removed. Given the difficulties of distilling an oxygenated mixture, a packed bed adsorber is a promising approach to achieve this separation.

When trying to understand the behavior of a complex mixture, it is useful to select model compounds that behave similarly to their compound groups and run experiments on them alone. Two main model compounds were selected: Acetic acid to model acetic acid and light oxygenate behavior, and m-cresol to model phenolic behavior. Experiments were conducted to study the separation of m-cresol from acetic

acid in a mixture. Activated carbon separates m-cresol from acetic acid quite effectively. When a stage 1 sample was analyzed, the bed separated the phenolics as well, but did not exhibit the same degree of separation as the model compound mixture.

Chapter 1: Introduction

1.1 Introduction to Biofuels

One of the few constants in modern life is the need for energy. From lighting and other household needs, to transportation and agriculture, the modern global economy requires significant energy resources to function and raise the standard of life around the world. Currently a significant portion of energy production, especially in the transportation sector, is produced via combustion of petroleum based fuels. While these resources currently supply the world with affordable and accessible energy, there are finite reserves of oil and gas within existing reservoirs. Resources that took millions of years to form are being consumed in hundreds of years. To plan for future needs, new sources of energy must be found. Of particular interest is the United States transportation sector. The American transportation sector was created with liquid fuels in mind. Petroleum based liquid fuels have a few major advantages: they are energy dense, the technology to utilize them is mature, and fuel tanks can be rapidly refilled. As such, an extensive network of distribution has been created for liquid fuels and the vast majority of vehicles are designed to burn them. This dynamic creates a great opportunity for biofuels. Biofuels share many of the same advantages as the petroleum based liquid fuels, but are also a renewable resource. If waste plant material could be converted to fuels, replacing non-renewable liquid fuels would be a much simpler endeavor. One potential method of converting biomass to fuel precursors is thermal decomposition, also known as pyrolysis.

1.2 Pyrolysis and Torrefaction Overview

Pyrolysis is the process of heating in an anaerobic environment [1, 2]. When solid biomass particles are pyrolized, they decompose into a mixture of oxygenated organic compounds that enter the vapor phase within the reactor; these compounds are highly oxygenated and do not have similar functionalities and carbon numbers as most fuel range molecules. This vapor phase can theoretically be subsequently upgraded, or first condensed into bio-oil and then upgraded. The resulting solid product remaining in the reactor is char.

To understand where each compound group produced comes from, it is useful to first understand the nature of biomass. Biomass is a lignocellulosic material. Three biopolymers make up all of biomass: lignin, hemicellulose, and cellulose [1, 3]. Each of these three biopolymers begins to decompose within a different temperature range and decomposes to a few unique functionalities; these ranges can be observed in the figure below [1, 3, 4]. A staged approach might aid in upgrading by segregating unique functionalities within a single thermal decomposition stage. This process is called torrefaction.

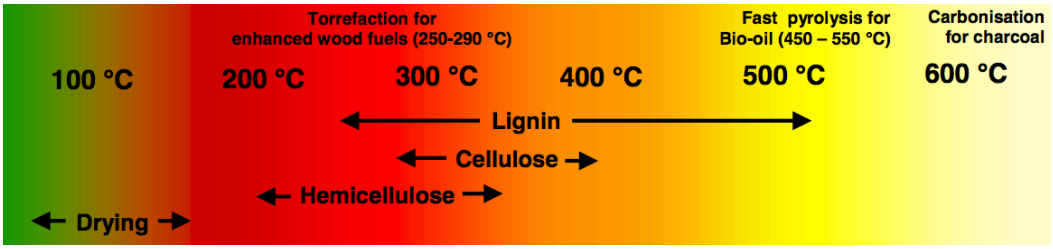

Figure 1. Temperature ranges in which hemicellulose, cellulose, and lignin decompose [3]

Examining these temperature ranges, hemicellulose should react at the lowest temperatures and form acetic acid and other light oxygenates, furans, pyrans, and

furfurals [3, 4]. One proposed set of stage 1 reaction conditions is a temperature of 270°C and a residence time of 20 minutes [4]. Cellulose should react at intermediate temperatures and form levoglucosan as well as other anhydrous sugars [3, 4]. The conditions chosen for stage 2 are a temperature of 350°C for 3 minutes [4]. Lignin decomposes at the highest temperatures and should form phenolic compounds [3]. A final fast pyrolysis stage is used at a temperature of 500°C for 1 minute to decompose all remaining material [2, 4, 5]. In addition to the compounds mentioned above, water is both produced from the decomposition reaction and evaporated from wet biomass; carbon dioxide is also formed. The figure below illustrates the torrefaction process.

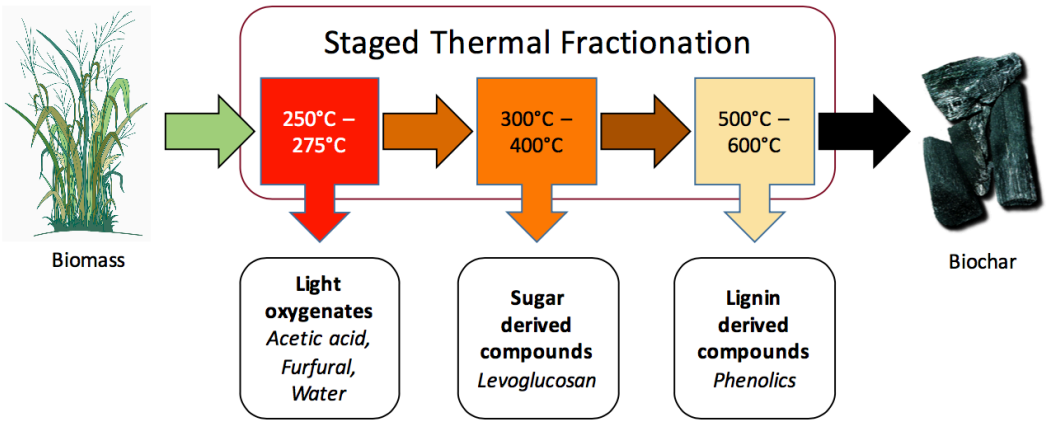

Figure 2. Theoretical torrefaction product distributions [4]

Unfortunately, torrefaction is not as selective as is desired. Lignin has a very broad range of temperatures at which it decomposes based on the various forms of lignin present as well as lignin bond functionalities [4]. A product distribution of the first stage of torrefaction of oak biomass is given below.

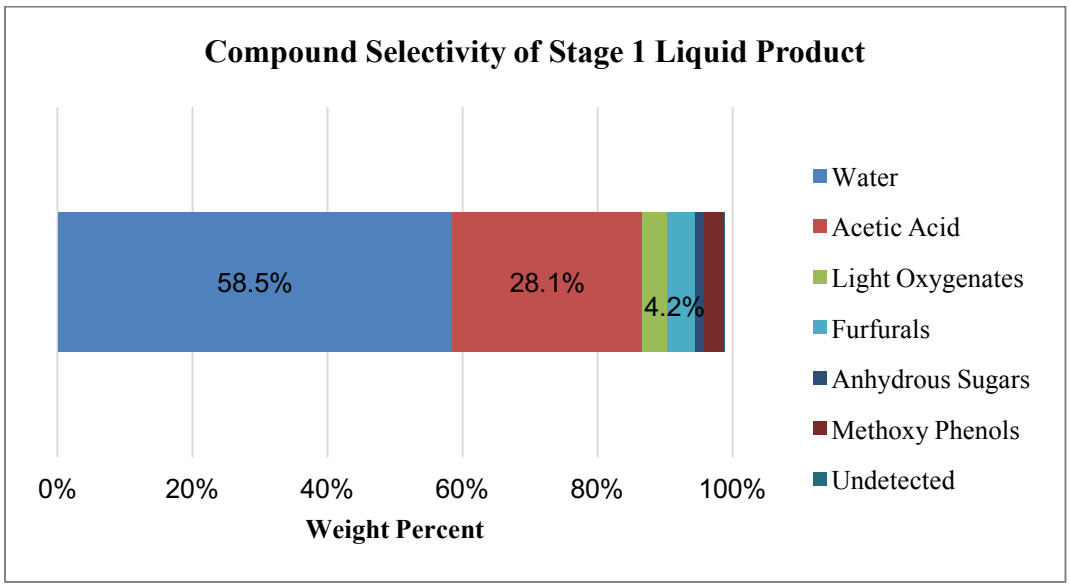

Figure 3. Stage 1 torrefaction of oak product selectivity [6]

Over 58% of the stage 1 liquid product is water (recall that not all of this water is a reaction product). Water is not useful for the production of fuels as it is a combustion reaction product. The water will ultimately need to be removed from the product stream. A more illuminating figure illustrating the compound selectivity excluding water is given below; these are the organic compounds and compound groups that can be upgraded into fuel molecules.

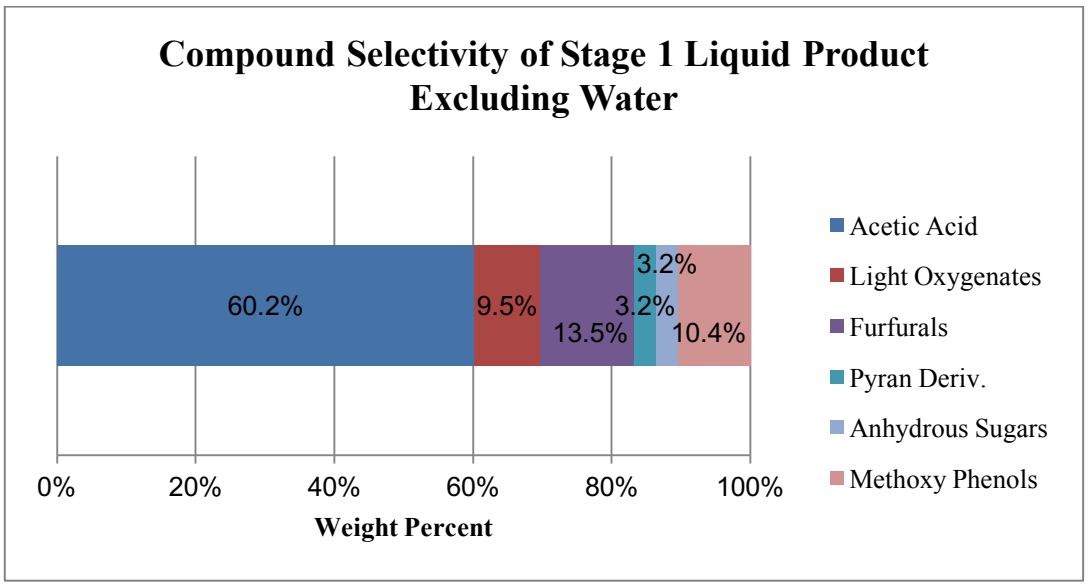

Figure 4. Stage 1 torrefaction of oak product selectivity excluding water [6]

About 60% of the stage 1 liquid is acetic acid, and another 26% is other light non-aromatics, but around 10% is lignin-derived phenolics and 3% is cellulose-derived anhydrous sugars. Stage 1 torrefaction selectivity is not particularly high which complicates any subsequent upgrading strategy.

1.3 Torrefaction Product Upgrading

While there is more than one strategy for upgrading stage 1 products, the majority involve a ketonization step [6]. As previously illustrated, over sixty percent of the stage 1 torrefaction liquid excluding water is acetic acid, and some of the other molecules are carboxylic acids as well. In a ketonization reaction, two carboxylic acids react to from a ketone, a carbon dioxide molecule, and a water molecule; in the case of two acetic acid molecules, acetone is formed [7, 8]. This reaction is generally conducted on TiO_2 or Ru/TiO_2 catalysts, which are far cheaper than a noble metal catalyst needed to conduct a hydrogenation step [7, 8]. After the ketonization step, acetone can be hydrogenated forming isopropanol or it can be made to react with itself

in an aldol condensation reaction to form molecules that can be added to or substitute for gasoline range hydrocarbons [7]. Alternatively, the acetic acid can be hydrogenated to form ethanol over a ruthenium or rhenium supported metal catalyst. Either way, the catalyst is deactivated rather rapidly as the reaction progresses. This deactivation is mostly due to coking of phenolic molecules but can also be caused by coke formation created by the deoxygenation of furan and anhydrous sugars such as levoglucosan [9, 10]. Coke deposits can cover active sites on the surface of the catalyst preventing adsorption and subsequent reactions at that site lowering the catalyst activity. Also, in the case of a porous catalyst, coke deposits can form near a pore mouth, causing pore closure; this coke blocking entry to the pore prevents access to all internal active sites, again reducing catalyst activity [9, 11]. In order to increase catalyst life, separation of the lignin-derived phenolic products would ease the task of upgrading stage 1 liquid to useful fuel molecules.

1.4 Separation by Adsorption

Given that some form of separation is necessary, an effective method must be found. Distillation is usually preferred as a method of separating a mixture based on the boiling points individual components. Unfortunately, that is not an option for the torrefaction liquid product as additional heating accelerates a polymerization reaction creating molecules far too heavy to be useful for fuels [7]. Adsorption on a packed bed could provide a solution to this difficulty.

When selecting an adsorbent, several factors must be considered. The adsorbent must have a large capacity per unit weight, phenolic compounds must adsorb relatively

strongly on it, and it must be either inexpensive to purchase or produced easily from raw materials. Activated carbon is an excellent choice.

Activated carbon can be created from many different natural materials including but not limited to wood, nutshells, and coal [12, 13]. This process contains two stages: carbonization and activation. In the carbonization step, the carbonaceous material is heated in an inert environment to a temperature under 800°C; this process removes non-carbon elements found in the raw material including hydrogen, oxygen, sulfur, and nitrogen [14]. Ultimately, this first step creates a porous structure within the particles but these pores are undeveloped and frequently inaccessible [14]. In the activation step, the particles are exposed to an oxidizing environment (carbon dioxide or steam) between 950°C and 1000°C that clears many of these pore blockages leaving a random distribution of pores of many sizes [12-15]. This process makes the char exiting stage 3 seem a promising raw material; the energy to carbonize it has already been input through the torrefaction process and there is likely no additional carbonization needed. Oxidization could potentially occur after packing an adsorbent bed full of char. Even if this possibility is difficult, activated carbon remains a very cheap substance to purchase.

The physical properties of activated carbon also make it a good selection for an adsorbent. Activated carbon has a very large surface area of 800-1500 m^2/g; this surface area is essentially fully within the many pores in a particle [13, 14]. Three types of pores exist in activated carbon: micropores with radii under 2nm which make up 95% of the surface area, mesopores with radii between 2nm and 50nm which make up 5% of the surface area, and macropores with radii greater than 50nm which do not

significantly contribute to the surface area [14]. The active sites which compounds adsorb to are contained within these pores.

Activated carbon is used regularly as an adsorbent to purify a mixture. One of the many common uses is to purify drinking water [12, 14]. Activated carbon has been shown to reliably adsorb phenolic molecules from a water mixture [12]. While acetic acid does adsorb, phenolic adsorption should be far stronger; when acetic acid is in adsorption/desorption equilibrium on or near a site, it can easily be replaced at that particular site by a phenolic forming a stronger interaction with the site [12, 16]. An activated carbon bed is also useful as, depending on the temperature of the bed, it can cause the condensation and thus separation of levoglucosan. Because of a combination of these factors, activated carbon is an excellent adsorbent to use for this process.

1.5 Scale Up Considerations

Ultimately, any system designed to adsorptively separate a stage 1 liquid must be able to flow on a continuous basis; non-continuous reactor feed streams cause unsteady-state operating conditions making reactor operation and optimization a greater challenge. Any scale up design operates on the principle that acetic acid and other light oxygenates do not adsorb strongly and flow through the bed. Phenolics adsorb more strongly but also can desorb depending on the bed conditions; when the phenolic needs to be extracted, the activated carbon could be maintained at the same temperature and the phenolics would slowly desorb. Alternatively, the bed could be heated which should speed desorption but would also increase the rate and favorability of a polymerization reaction.

Two potential scaled up designs are a temperature swing adsorption setup using two or more packed beds or a continuous regeneration moving bed. A design using multiple beds is illustrated in the figure below.

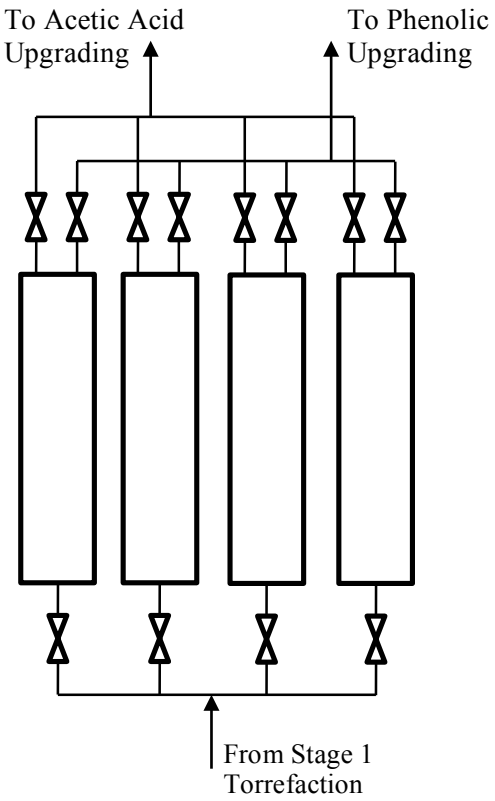

Figure 5. Adsorptive separator using multiple beds

In the design using multiple beds, one bed would be connected to the stage 1 product stream and the ketonization reactor and all others would be desorbing separated phenol, probably at a higher temperature and flowing to a different reactor. After completing the desorption of phenolic molecules, the second parallel bed would be allowed to cool. When phenolic molecules begin to break through the first bed, flow from the torrefaction unit and to the upgrading reactor would be switched to the second bed; the first bed would be heated to desorb the adsorbed phenolics. The number of

beds would be determined by the difference between the time it takes for phenolic molecules to transit an activated carbon bed and the amount of time it takes for them to desorb and be removed. One potential drawback of this process is it does not necessarily provide a steady state flow to a reactor unless there is an acetic acid holding vessel between the ketonization reactor and the adsorbent bed.

The second possible design involves a moving bed. In this case, the activated carbon would flow countercurrent to the flow of stage 1 product; this would maintain a constant concentration profile along the bed and require only a single bed. As the activated carbon nears the bed entrance, the adsorbed concentration of phenolic molecules reaches a maximum; it is then removed from the bed for phenolic desorption and recycled to the bed outlet for reuse. Moving bed technology yields a steady-state stream for subsequent upgrading and is quite mature as it is used industrially in naphtha reformers to allow for constant catalyst regeneration [17].

Chapter 2: Adsorptive Separation on a Packed Bed

2.1 Experimental Techniques

2.1.1 Experimental Techniques Using SRI GC

To conduct analysis on liquid samples, a SRI 8610C Gas Chromatograph with a flame ionization detector (or FID) was used. The column used inside the GC was made out of a 27 cm long length of 1/8 inch OD stainless steel tubing. The inside of the column was packed with 120 mg of 20-40 mesh Darco activated carbon marketed by the Aldrich Chemical Company and sold by Sigma Aldrich. The ends were packed with non-adsorptive glass wool to ensure no loss of the adsorptive media. To ensure there were no air pockets and complete packing of column, the column was held on end and vibrated. The column was then bent with a gentle radius to fit inside the column oven on the GC. This column can be seen in the figure below. All experiments were conducted with a nitrogen carrier gas flow rate of 70 mL/min. Gas flow rates were checked regularly.

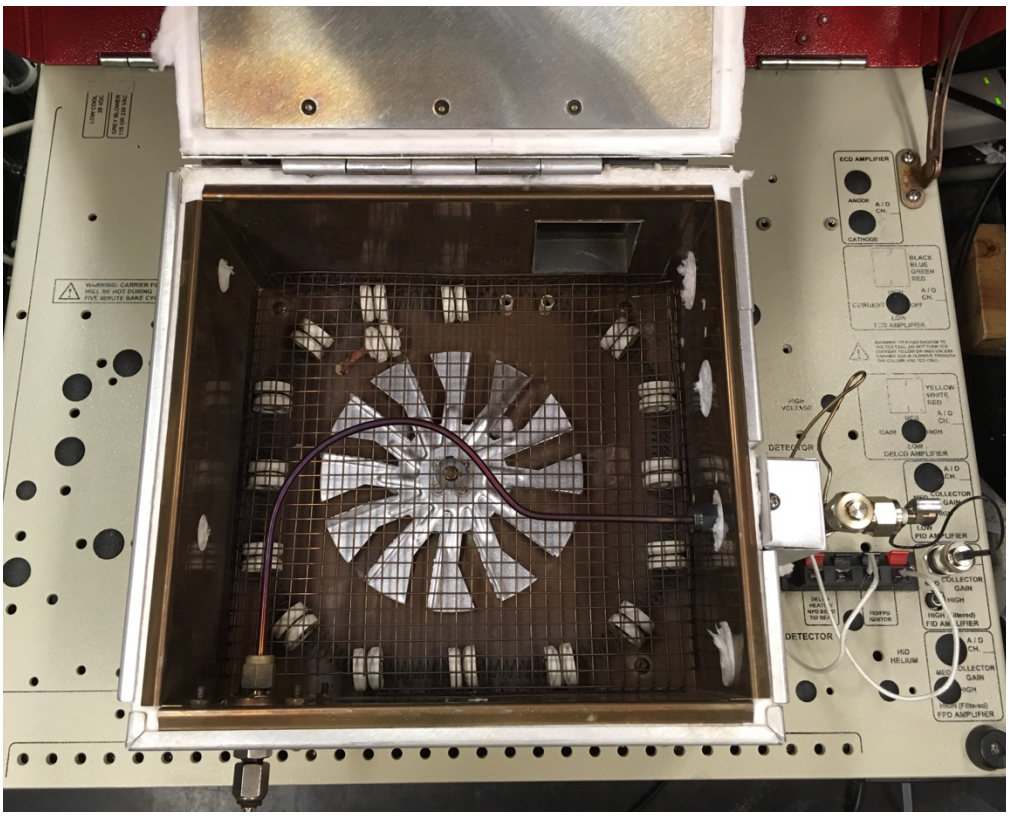

Figure 6. Photograph looking down towards open GC oven.

Compounds were injected with a 10µL Hamilton syringe. Anytime a liquid was first drawn into the syringe, a bubble of approximately 0.7 µL would form between the plunger and the liquid. To eliminate this air bubble in the syringe, the plunger was repeatedly pushed in and out while the tip of the needle was in the liquid contained in the GC vial. This technique ensured repeatable injection volumes. After each liquid injection, the syringe was rinsed with acetone; the acetone was allowed to evaporate between each trial. A minimum of 3 trials were conducted for each sample. At the end of each trial the column was baked out at 350ºC to ensure desorption and outflow of all compounds from the prior trial.

At the beginning of each trial, a 5µL volume of methane was injected into the column to confirm proper FID function. If need be, to confirm that the FID was lit, a wrench would be held near the outlet to observe condensation (formed by water vapor produced by combustion reaction). A schematic of the GC is illustrated in the figure below.

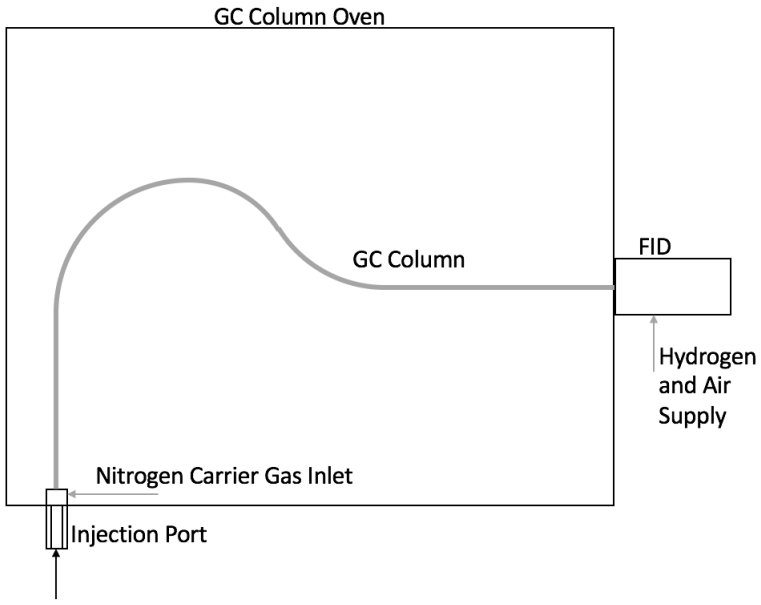

Figure 7. SRI GC schematic

2.1.2 Calculation of the Peak Areas

SRI provides software to receive data from the instrument and create the chromatogram: Peak Simple. This software contains a peak integration tool that determines both the retention time and peak area of each individual peak; however, the software was designed for narrow peaks characteristic of very small samples. As such, the software does not hold the base line of integration at the base of the peak (a 0mV signal). This is illustrated in the figure below.

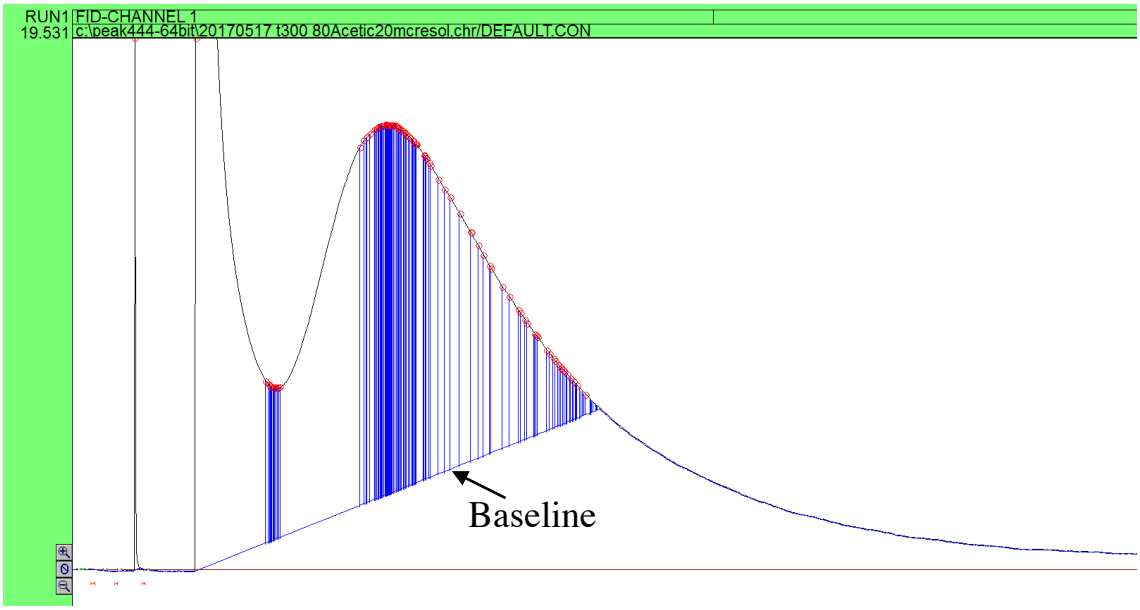

Figure 8. Peak Simple chromatogram prior to adjusting baseline

In the above figure the baseline automatically determined by Peak Simple travels up to meet the decreasing signal on the tail end of the peak. The vertical blue lines denote individual peak boundaries and the red circles the individual peaks identified by the software. To correct for this, the manual integration tool must be used to keep the baseline of integration at 0 mV and then all the individual peaks identified can be summed in Excel to find the actual peak area. To determine which peak areas on the border between the two adjacent peaks are added to each, the chromatogram was zoomed in tightly to estimate the boundary; then the areas of the small peaks were added to the corresponding adjacent peak's peak area. The corrected baseline is illustrated in the figure below.

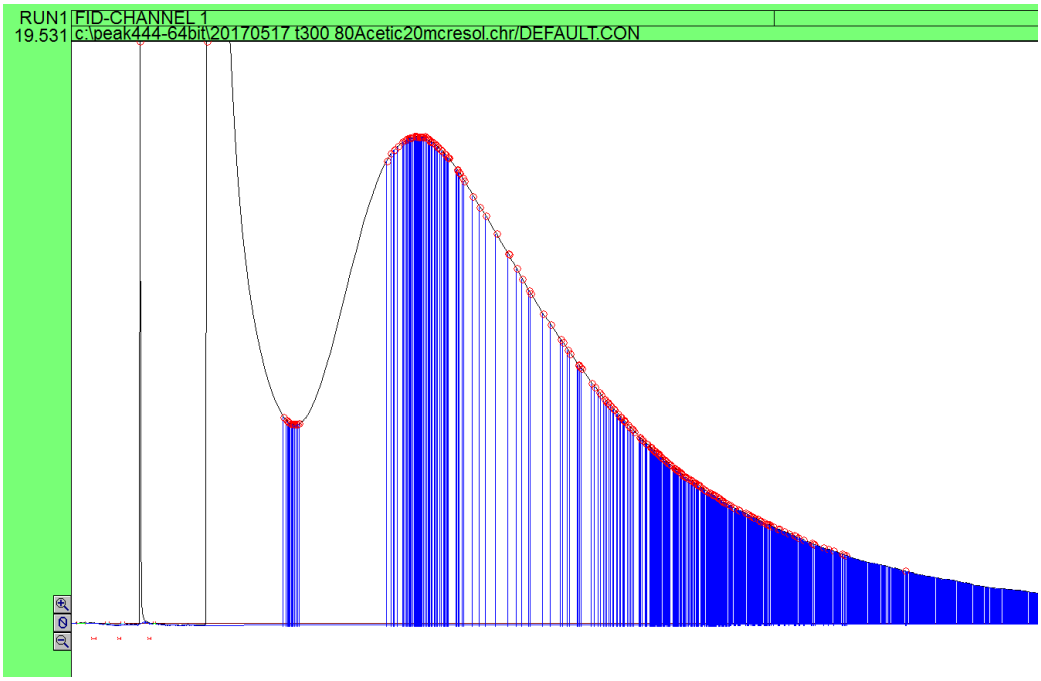

Figure 9. Peak Simple chromatogram after correcting baseline

The baseline correction will not eliminate all error contributions of this integration process. On the tailing edge of the peak, many peak boundaries are identified by a vertical blue line; however, the Peak Simple software does not always identify the area within the trapezoid formed by the two peak boundaries, peak, and baseline as an individual peak and report its peak area. This only occurs when the detector signal (the y-axis) is less than 2.5 mV. During most of these experiments, this will contribute a relatively small amount of error given some peaks reach 5500 mV on the y-axis; nonetheless, it must be considered.

In conducting an error analysis throughout this document, 90% confidence intervals are used based on a t-distribution due to the relatively low number of trials for each experiment.

2.2 Model Compound Selection

2.2.1 Model Compounds Selected and Rationale

In order to be able to understand the behavior of a multicomponent liquid, it is often convenient to select a few model compounds to study. The model compounds selected must approximate large fractions of the mixture. In the case of stage 1 torrefaction liquid, acetic acid is an obvious choice to use to study the acetic acid and light oxygenate behavior. To study the phenolic behavior, m-cresol was selected. m-Cresol is an alkyl phenol that is one of the least oxygenated and smallest phenolic components in the stage 1 liquid. As such, the strength of its adsorption to activated carbon will likely be lower than other phenolic compounds and thus it will have one of the shortest retention times in the phenolic compound group. m-Cresol, therefore, ought to present the boundary condition for adsorptive separation as it would be the first phenolic compound to elute. Additionally, m-cresol is a good choice because of it has several industrial uses and is not an uncommon compound.

2.2.2 Experimental Conditions

Experiments were conducted at 300ºC. This temperature was selected as it appears to be a temperature sufficiently high to prevent significant acetic acid adsorption. A temperature significantly higher than this will accelerate the rate of undesirable side reactions like polymerization and also require more heating energy in a scaled up facility. If the acetic acid retention time is not minimized, the steady flow of acetic acid and other light oxygenates to subsequent upgrading reactors will experience greater fluctuation and lead to more unsteady state conditions within those reactors.

2.2.3 Model Compound Neat Injections

The behavior of each individual compound must be first characterized. Neat (pure compound) injections were conducted on the activated carbon column in volumes sufficient to prevent saturating the detector while still maintaining a sufficiently large injection volume to be repeatable. If the detector is saturated, the top of the peak will be truncated, leading to inaccurate peak area measurements. Acetic acid was injected in volumes of 0.5 µL and m-cresol was injected in 1.0 µL volumes. A minimum of 5 injections of each sample was conducted in the neat model compound study to ensure greater confidence in the repeatability of this data. An acetic acid peak and m-cresol peak are displayed in the figures below.

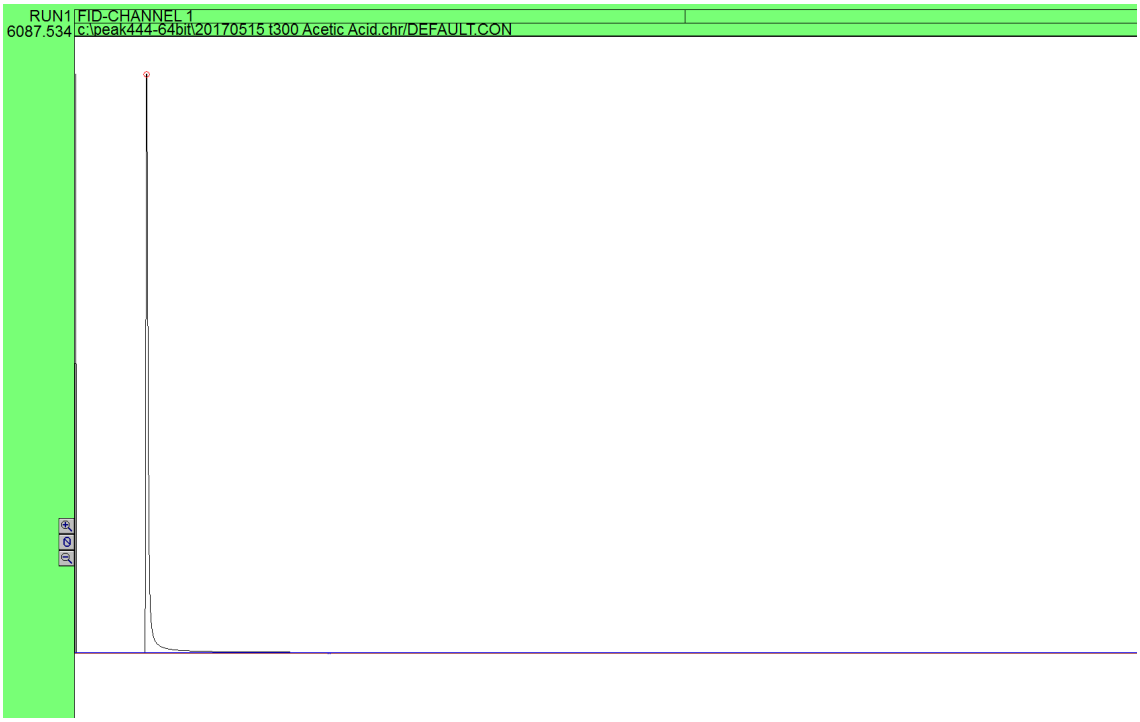

Figure 10. Neat 0.5 µL acetic acid peak at 300°C

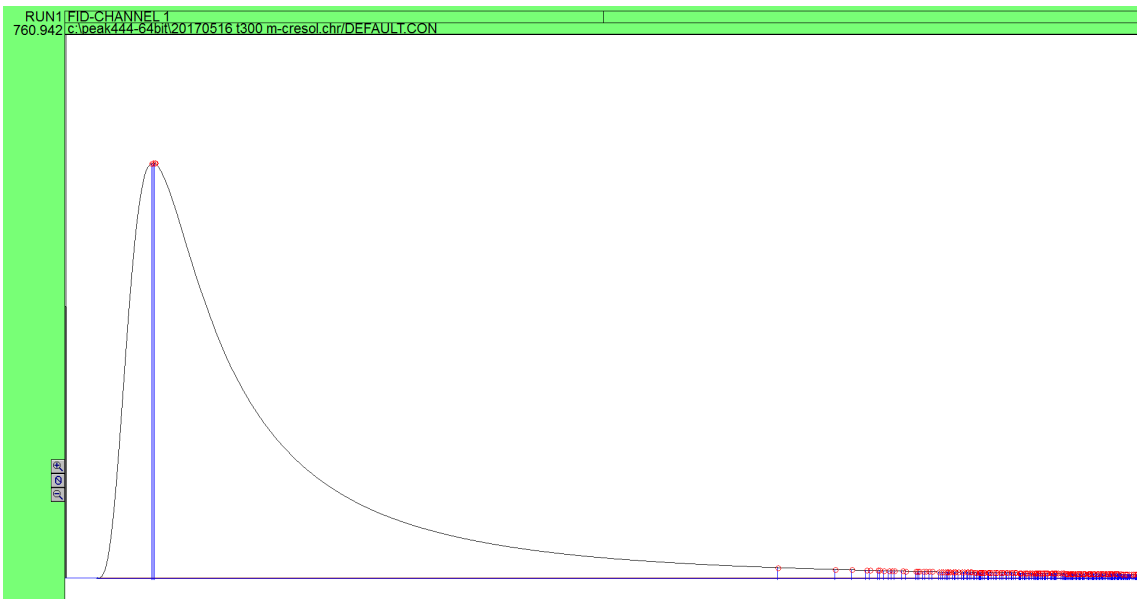

Figure 11. Neat 1 µL m-cresol peak at 300°C

The retention times and peak areas of these compounds are illustrated in the figures below. Retention time is the amount of time between the injection of a compound onto the column and the maxima of the peak; the peak maxima is the moment when more compound is exiting the column then at any other time.

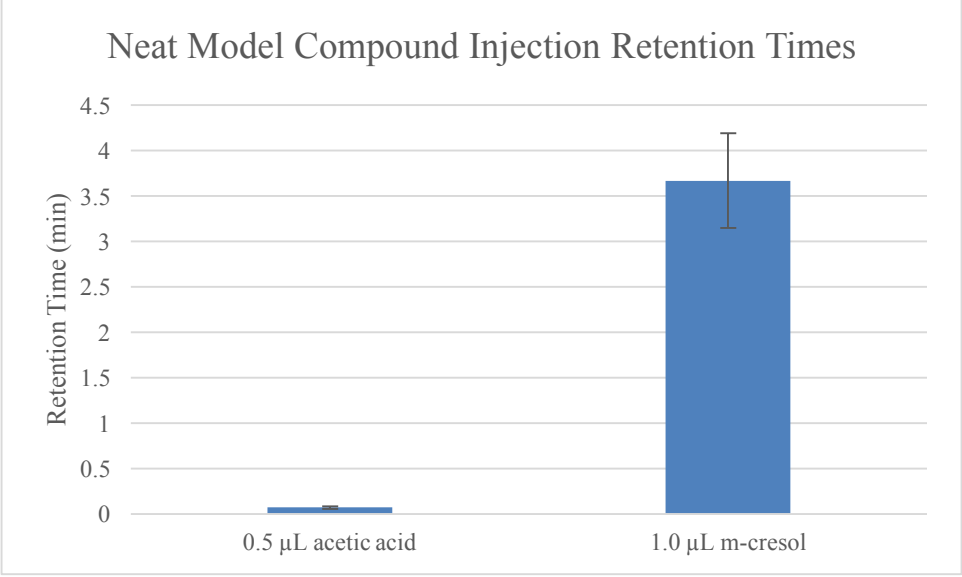

Figure 12. Neat model compound retention times at 300°C

As seen above, the retention time of acetic acid on the activated carbon bed is 0.07±0.01 minutes and the retention time of m-cresol is 3.7±0.5 minutes. The methane retention time is 0.03-0.04 minutes and methane is nonadsorbing. The acetic acid adsorbs weakly and its elution is only slightly slower than the nonadsorbing methane. m-Cresol has a significantly longer retention time and therefore should separate well from the lighter components in a mixture. This behavior is expected; the phenolic should adsorb far more strongly than acetic acid. One of the assumptions in chromatography is that a compound within a mixture should behave similarly to when it is alone within a chromatographic column. If this assumption is correct in this case, neat injections would suggest a high degree of separation could be achieved in a larger bed or scaled up design due to the difference in retention time.

2.3 Binary Mixtures

2.3.1 Low Volume Binary Mixture Injections

A binary mixture of acetic acid and m-cresol should demonstrate similar adsorption and separation behavior as the stage 1 liquid. A 20% m-cresol 80% acetic acid ratio was selected as this should be the upper limit of the phenolic to acetic acid/light oxygenate ratio in the stage 1 torrefaction liquid. The injection size was 0.5 μL to avoid saturating the detector with acetic acid. The results of these trials are presented in the figures below.

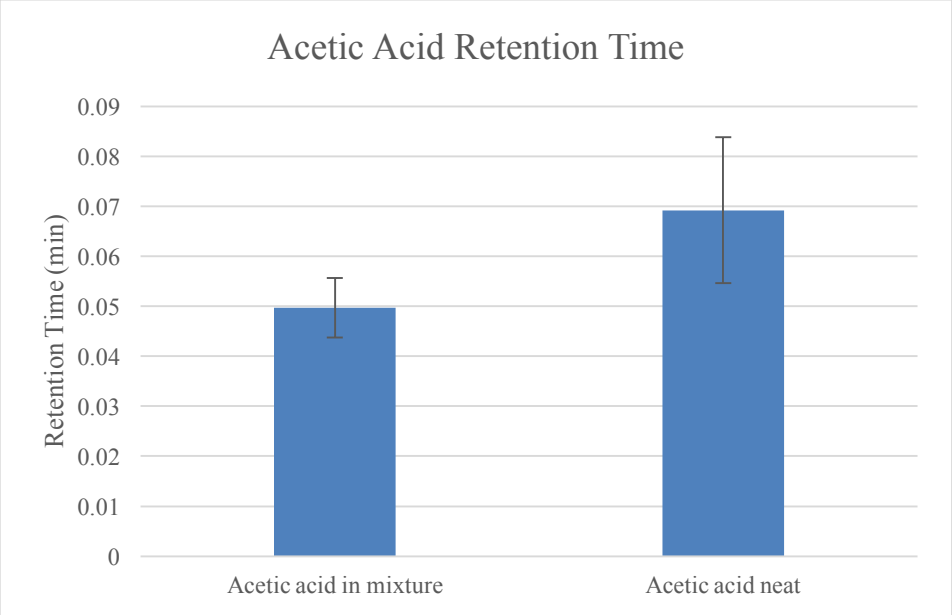

Figure 13. Acetic acid retention times in a binary mixture and neat

There is no statistically significant difference between the retention times in a mixture and neat for acetic acid. A very different result is reached for m-cresol.

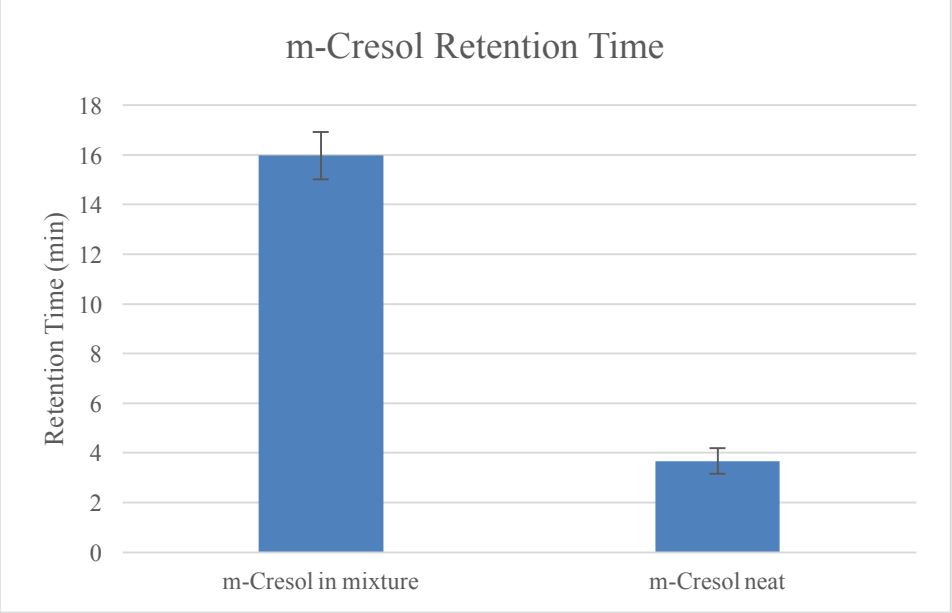

Figure 14. m-Cresol retention times in a binary mixture and neat

The retention time of the m-cresol in the binary mixture is 16.0±1.0 minutes while the retention time of the neat m-cresol is 3.6±0.5 minutes. There are two hypotheses for these discrepancies:

1. There are at least two types of sites on the activated carbon. One type of site selectively adsorbs acetic acid; adsorbed acetic acid molecules forms hydrogen bonds with m-cresol molecules. Hydrogen bonding between adsorbed acetic acid and m-cresol in the bulk phase and in the pores slows the travel of m-cresol through the column causing the additional retention time.
2. There are at least two types of sites on the activated carbon. One type of site allows m-cresol to adsorb very strongly but there are relatively few of this variety of site per gram of activated carbon. m-Cresol desorbs slowly from these sites. Given the low number of these sites, low volumes of m-cresol will travel slowly down the column while higher volumes will travel more rapidly.

2.3.2 Binary Mixture Using Hexane

To test the first hypothesis, the acetic acid was replaced by hexane giving an 80% hexane, 20% m-cresol binary mixture. Hexane should not adsorb strongly and cannot form hydrogen bonds and therefore its intermolecular interactions with m-cresol should be limited to Van der Waals interactions. Only two trials were conducted. The results of this are given in the figure below.

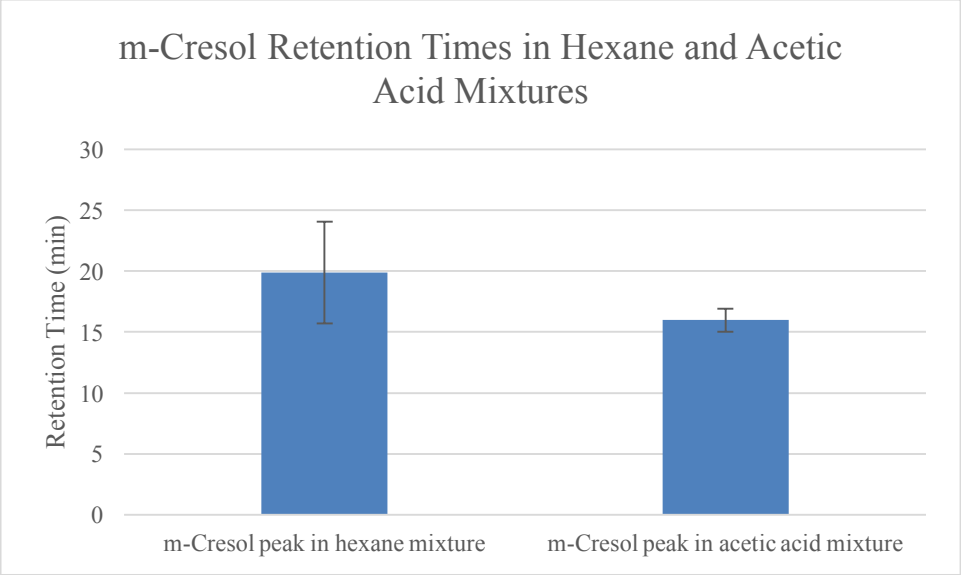

Figure 15. m-Cresol retention times in hexane-m-cresol and acetic acid-m-cresol mixtures

The retention time of m-cresol in the hexane-m-cresol is greater than in the acetic acid mixture; it certainly is not close to the 3.7 minutes of the neat injection. Therefore, hypothesis one is rejected.

2.3.3 Large Volume Binary Mixture Injections

To test the second hypothesis, 1 µL of m-cresol in the mixture will be used as was used in the neat injection necessitating a 5 µL injection of the acetic acid-m-cresol mixture. Given a similar volume of m-cresol, any behavior by the very strongly adsorbing sites would not be as significant a contributor given the ten times larger volume. The results are presented in the figure below.

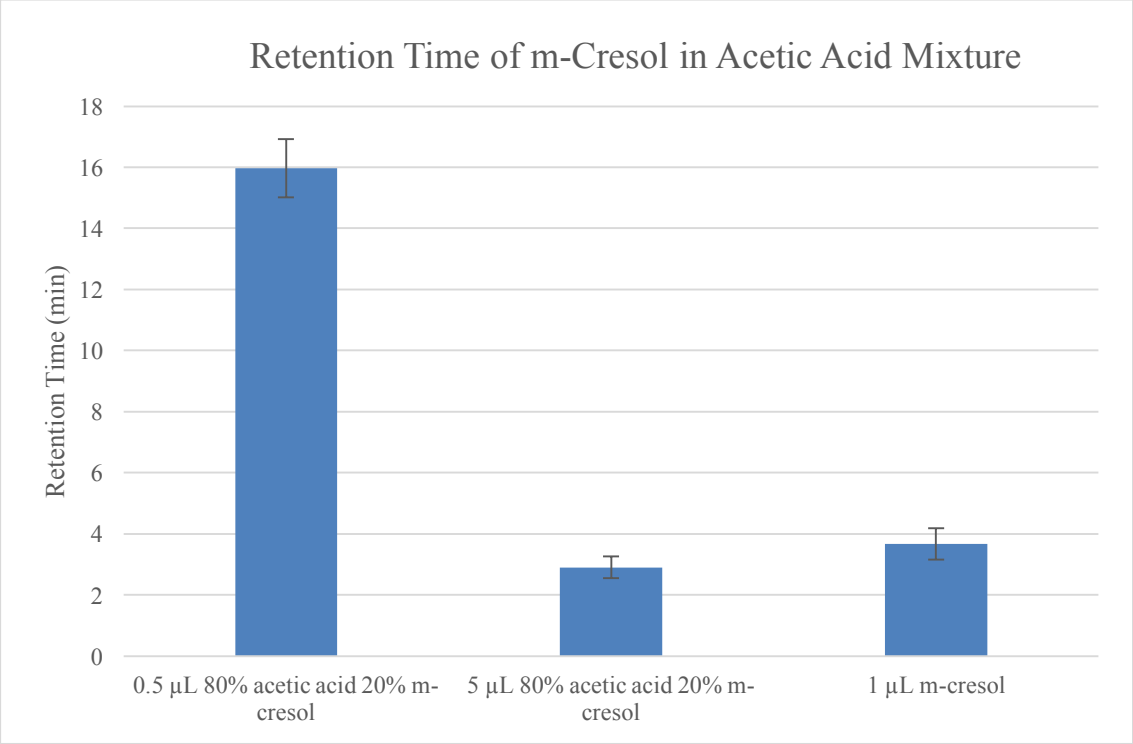

Figure 16. Retention time of m-cresol in acetic acid-m-cresol mixture

The retention time of the 5 µL sample was 2.9±0.4 minutes. While this is less than the 1 µL neat m-cresol retention time of 3.7±0.5 minutes, this difference is easier to explain. Given 4 µL of acetic acid in the mixture, it is likely that there is some competitive adsorption on sites, reducing the number of sites available for m-cresol molecules to adsorb, which would reduce the retention time. This would seem to confirm hypothesis two. Additionally, the question presented by the reduced areas of the 0.5 µL of the acetic acid mixture is resolved as well.

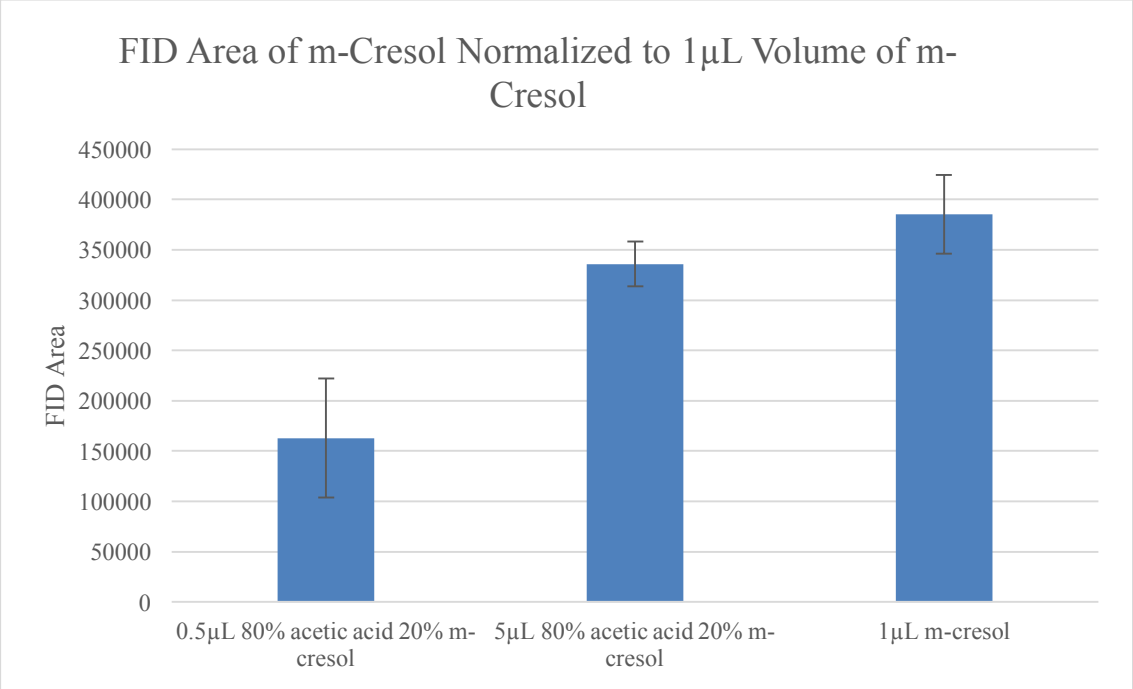

Figure 17. FID area of m-cresol normalized to a 1 µL volume of m-cresol

After normalizing the FID areas to a 1 µL volume of m-cresol, the 0.5 µL acetic acid mixture injection has peak area half the size of the neat m-cresol. This is likely caused by the smaller volume of m-cresol strongly adsorbing to a few sites and not desorbing relatively quickly. It will eventually desorb and be detected, but that signal would be so small it would be lost in the detector noise present on the tail end of a chromatogram.

In a larger design, sites that adsorb more strongly could be beneficial as they would allow for more time on stream before regenerating, but would not be likely to have a significant impact. Because of the small amount of extremely active sites and the high flow rates present in any industrial system, it is unlikely that this phenomenon would have an impact when scaled up. The model compound mixture behaved similarly to neat injections.

2.4 More Complex Mixtures

2.4.1 Ternary Mixtures Including Water

Over half of the stage 1 liquid is water; this presents a potential concern. Water should be a non-adsorbing compound and therefore should not affect adsorption or retention times of any compounds in the mixture, but this needed to be experimentally verified. Additionally, given that water is a combustion product and will not burn, it cannot be detected by the FID. A 50% water, 40% acetic acid, and 10% m-cresol solution was created and a 1 µL injection volume was used (ensuring same volumes of acetic acid and m-cresol injected as in previous experiment).

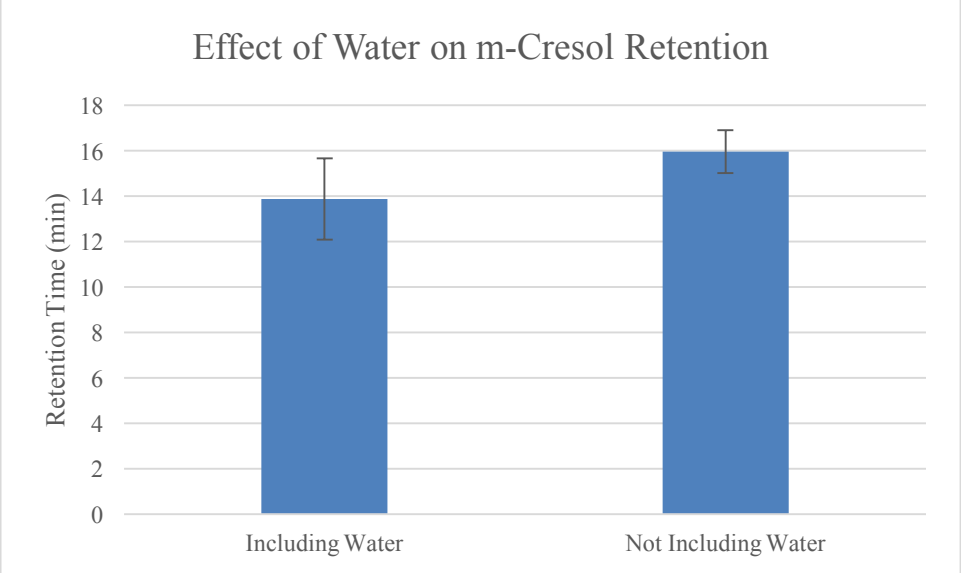

Figure 18. Effect of water on m-cresol retention

The retention time of the m-cresol peak in the 50% water solution is 14±2 minutes. This lower retention time could be due to the water preventing entry to pores on the activated carbon thus temporarily reducing the number of accessible sites. Also, the 90% confidence intervals are sufficiently large that there may be no statistically

significant difference between the two. Either way, there does not appear to be a very significant effect of water in the mixture.

2.4.2 Quaternary Mixture Including Methylfuran

Stage 1 liquid also contains pyrans, furans, and furfurals albeit in lower concentrations (normally about 5% of the total mixture). A model compound selected to test this was methylfuran. Methylfuran has a retention time between 0.1 and 0.2 minutes. It was difficult to determine the exact retention time because even a 0.1 µL injection saturated the detector. Either way, a compound with that retention time should not show up in a third peak but rather should elute along with the acetic acid. A 50% water, 35% acetic acid, 10% m-cresol, 5% methylfuran solution was prepared and injected in 1 µL volumes.

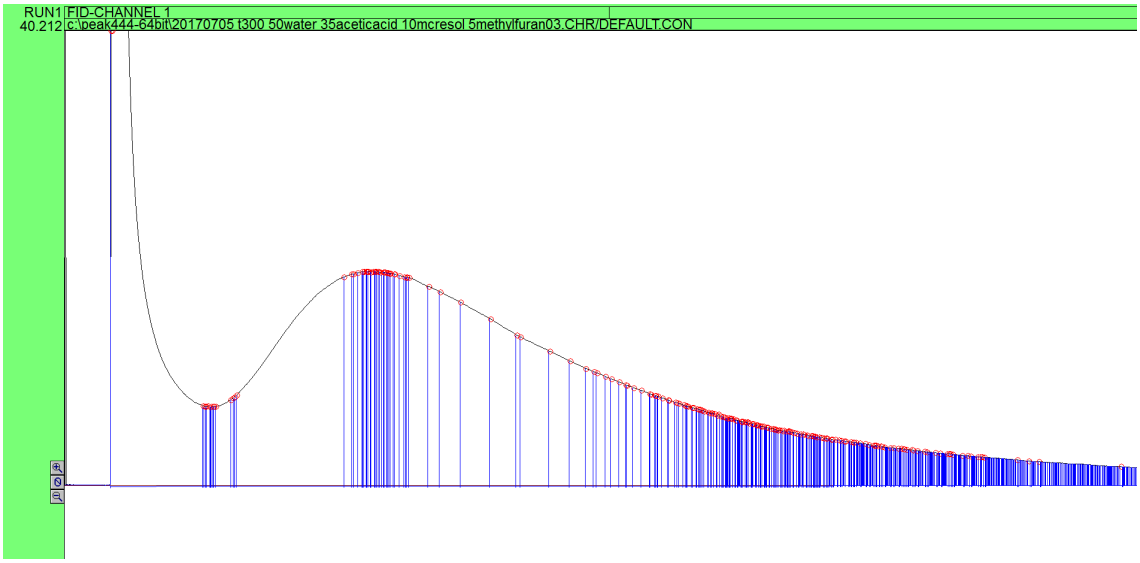

Figure 19. A chromatogram from one of the three quaternary mixture trials

This hypothesis was confirmed by the chromatogram. There is no third peak or shoulder. Additionally, methylfuran has minimal impact on m-cresol retention time as seen in the figure below.

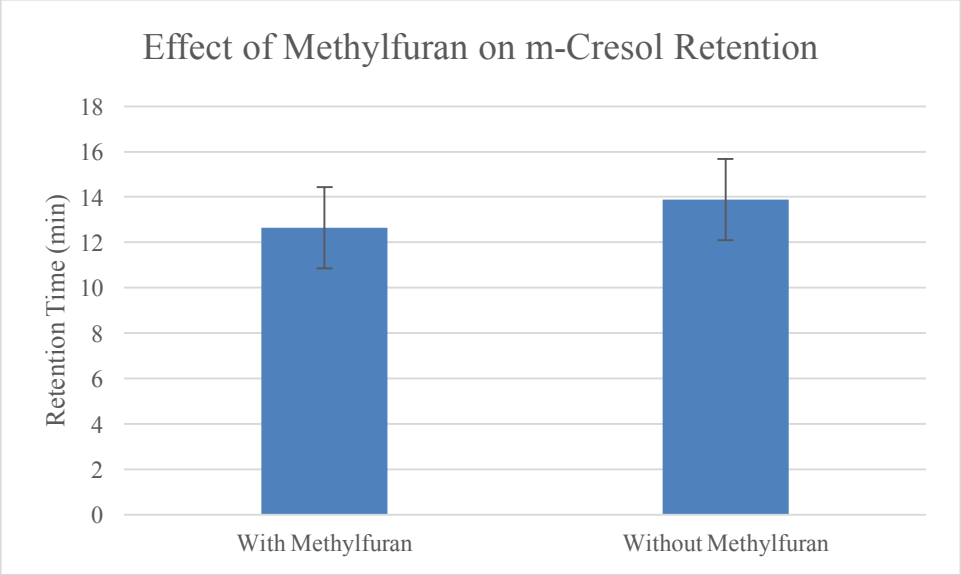

Figure 20. Effect of methylfuran on m-cresol retention time

Given the fact that only two peaks were present on the chromatogram, a neat injection of methylfuran was conducted to determine which peak it was contained within. Methylfuran's retention time places it within the first peak.

These experiments suggest that water need not be separated prior to flowing through the packed bed adsorber, allowing for it to be removed later in the upgrading process. This could be done through distillation; as the stage 1 product stream is further upgraded, it becomes less oxygenated making distillation to remove water a possibility. Because the activated carbon bed does not separate furans or furfurals, the catalyst used to upgrade the acetic acid stream must be able to tolerate these compound groups. This will lead to more coking than a pure acetic acid stream, albeit far less than prior to the removal of the phenolic compounds.

2.5 Stage 1 Torrefaction Liquid

2.5.1 Stage 1 Torrefaction Liquid Separation

The goal of the binary mixture and other model compound studies was to better understand how the adsorption on the activated carbon of the various compound groups in stage 1 liquid (displayed in figure 4) affects the separation. It is illuminating to study the stage 1 liquid separation and adsorption itself. The retention times of the acetic acid/light oxygenate peak and the phenolic peak are given below.

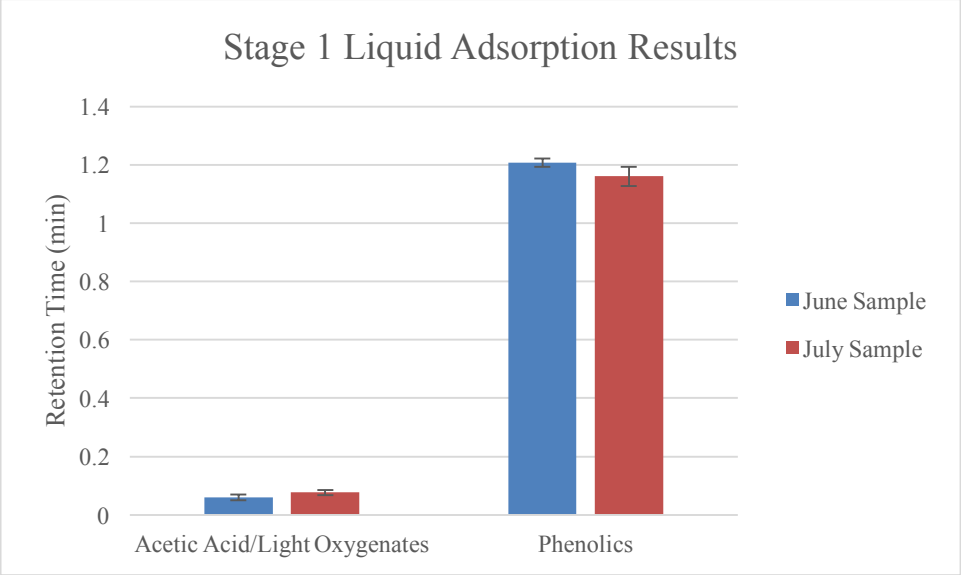

Figure 21. Stage 1 liquid retention times on activated carbon bed

The acetic acid/light oxygenate retention times are quite similar to the retention times observed of acetic acid in other experiments. The retention time of the phenolic is about three times faster than m-cresol. Two possible explanations of this discrepancy are:

1. There is levoglucosan in the stage 1 liquid that condenses on the activated carbon blocking pores.

2. m-Cresol adsorbs more strongly than the average phenolic molecule and is therefore not the best choice of a model compound.

Either way, this is an excellent avenue for future experimentation and analysis. It is also important to note that the degree of separation between the two peaks is less than in the acetic acid-m-cresol mixture for the same amount of activated carbon. The overlap between the phenolic peak and acetic acid peak is greater in the stage 1 liquid. This difference can be seen in the figures below.

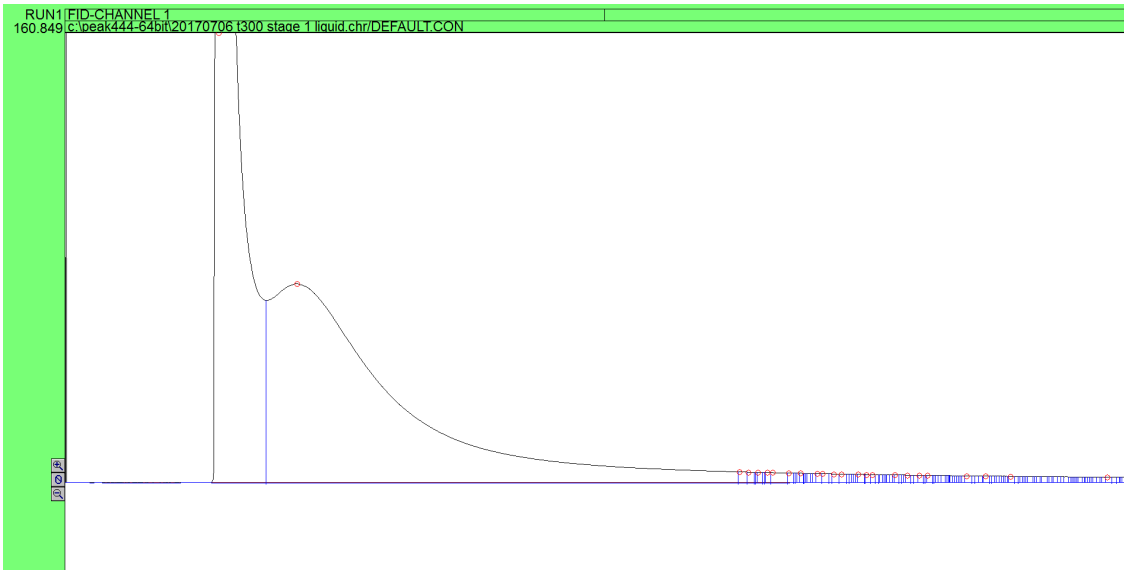

Figure 22. Chromatogram of 1 µL injection of stage 1 liquid

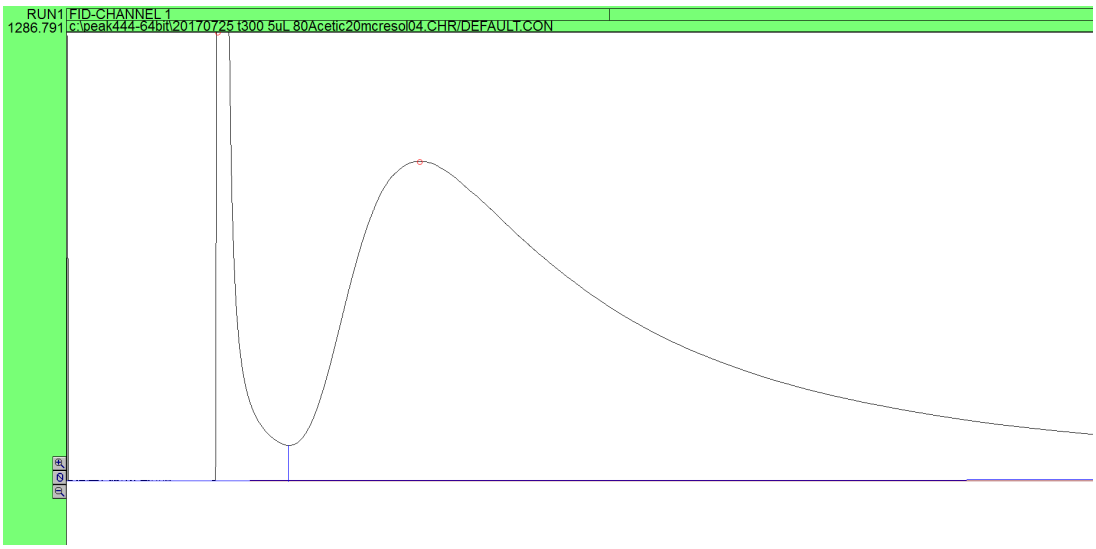

Figure 23. Chromatogram of 5 µL injection of acetic acid-m-cresol mixture

If stage 1 liquid is indeed more difficult to separate than the model compound mixture, more parallel beds will be needed or longer beds will be needed due to the reduced break through time for phenolics. In the case of a moving bed, adsorbent flow would need to be increased to ensure fresh adsorbent and more rapid phenolic removal.

2.6 Activated Carbon Deactivation

2.6.1 Activated Carbon Retention Time Decrease

During the final set of experiments conducted on the column, the 5 µL injections of 80% acetic acid, 20% m-cresol, an interesting trend emerged. The m-cresol retention times decreased and reached a plateau. This can be observed in the figure below.

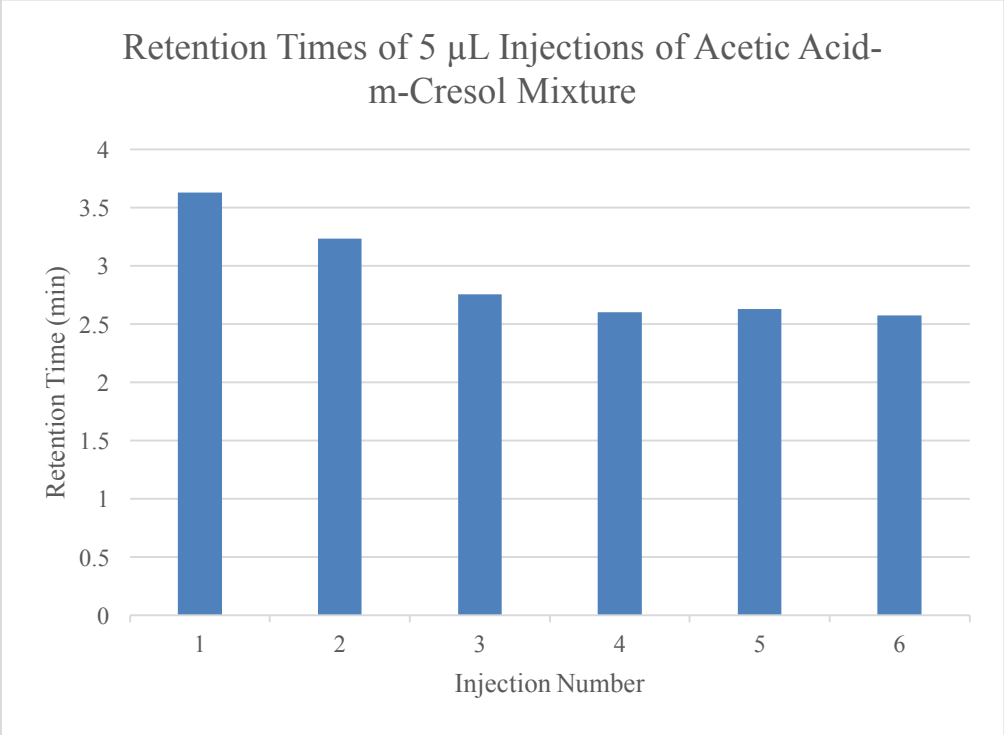

Figure 24. Retention times of 5 µL injections of m-cresol acetic acid mixture

An overnight bake out at 350ºC was conducted between all trials and a 60 hour bake out was conducted between the fifth and sixth injection. It seems that some sites within the activated carbon are no longer accessible, due to either permanent adsorption, coking, or pore closure. Either way, the higher retention time could not be restored. This behavior can also be observed in the decrease in the peak areas of the injections as well displayed in the figure below. The first and second peak areas are smaller due to some of the m-cresol never exiting the column and reaching the FID.

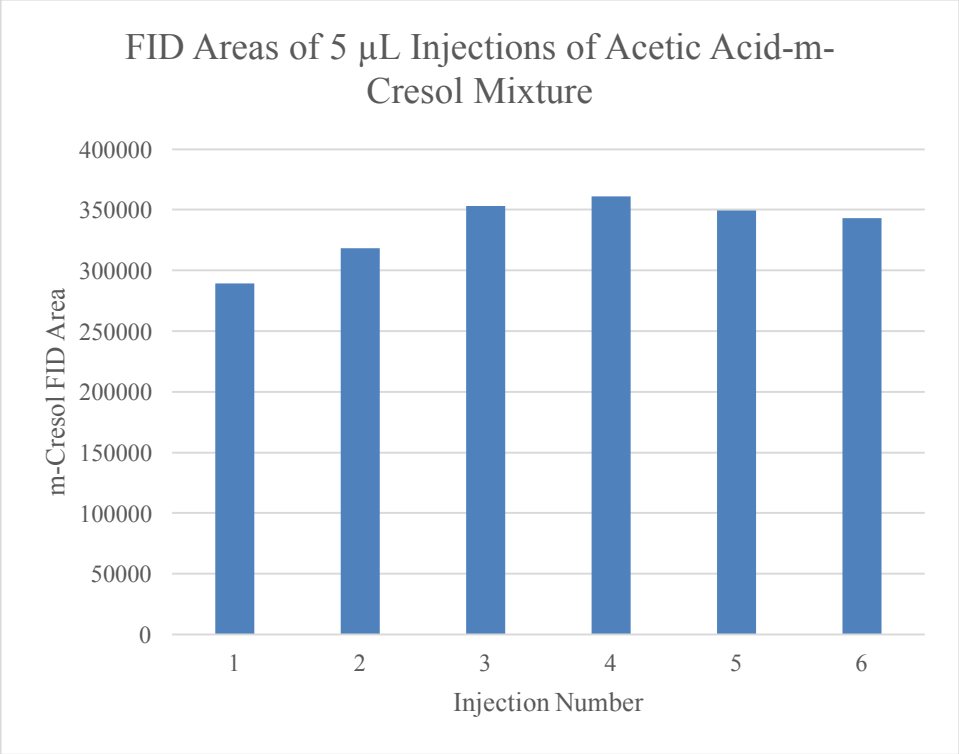

Figure 25. FID areas of 5 µL injections of acetic acid-m-cresol mixture

Further examination of the question of permanent adsorption provides an excellent avenue for future work. It would be illuminating to determine if the deactivation is caused by coking and ultimately pore closure; if so, the coke might be able to be removed or gasified and adsorbent activity and capacity restored. Additionally, a study of the effect of higher bake out temperatures on the time to desorb phenolics would be useful as this is an important parameter in a scaled up design given it partially determines the number of beds needed or the flow rate of activated carbon in a moving bed. This is currently difficult due to equipment limitations.

The current preliminary scale up does not consider the need for any regeneration beyond speeding the rate of desorption. Prior to this, potential scale up designs included either a moving bed or multiple packed beds. If the activated carbon adsorbent

is rapidly deactivated, the adsorbent would need to be removed for regeneration, regenerated in place, or even replaced if the method of deactivation is not coking. This makes the moving bed option look more promising as the adsorbent is constantly being removed from the bed due to the nature of the design. Alternatively, the passivation may not be reversible, especially if the beds are not heated for the desorption step. If this is the case, larger beds will be needed to account for this rapid capacity loss during the beginning of the adsorbent's life.

Chapter 3: Adsorption Modeling

3.1 Theory of Adsorption Modeling

3.1.1 Purpose of Adsorption Modeling

The ultimate goal of this adsorption research is to design a scaled up adsorptive separation unit. To be able to do this, a model must be developed; it is useful to first model adsorption on activated carbon on a small scale. A model with the same bed dimensions as used to conduct the experiments will allow for a comparison between the model's results and experimental data. Then, certain fundamental constants to the adsorption process used in the model can be adjusted to fit the model to experimental data. Fundamental constants for this process should be the same on the small scale and the large scale which will allow for the small scale bed to be accurately scaled up.

3.1.2 Primary Considerations of Modeling

Modeling adsorption in a packed bed separator can be a difficult task both to visualize and to conduct; therefore, it is useful to consider the similarity between a packed bed reactor (PBR) and this system. In a PBR at steady state, the concentration of the reactant (and product) varies with respect to position as the reaction converts the reactant to product. Several resistances slow this process: external mass transfer to catalyst surface, internal mass transfer within pore space, adsorption/desorption to reactive site, and the rate of reaction; these determine the concentration profile within the bed by resisting change [11]. A packed adsorbent bed separator is analogous but with one major difference: there is no reaction. This means that the adsorption of the adsorbate onto surface sites (resisted by mass transfer effects) directly causes the concentration gradient along the bed. This system is still not quite that simple given the

unsteady state conditions. Concentration will vary both with respect to time and position.

3.1.3 Useful Equations for Modeling Adsorption

Schneider and Smith propose a useful set of equations for modeling adsorption in porous media. They present a system of three simultaneous differential equations that can be used to determine bulk concentration with respect to time and position in the bed. These equations are stated below along with the external diffusion boundary condition and the variable meanings are defined [18].

$$\frac{E_a}{\alpha}\frac{\partial^2 c}{\partial z^2} - \mathrm{v}\frac{\partial c}{\partial z} - \frac{\partial \mathrm{c}}{\partial \mathrm{t}} - \frac{3D_c}{R}\frac{1-\alpha}{\alpha}\left(\frac{\partial c_i}{\partial r}\right)_{r=R} = 0 \qquad \text{Equation 1}$$

$$\frac{D_c}{\beta}\left(\frac{\partial^2 c_i}{\partial r^2} + \frac{2}{r}\frac{\partial c_i}{\partial r}\right) - \frac{\partial c_i}{\partial t} - \frac{\rho_p}{\beta}\frac{\partial c_{ads}}{\partial t} = 0 \qquad \text{Equation 2}$$

$$\frac{\partial c_{ads}}{\partial t} = k_{ads}\left(c_i - \frac{c_{ads}}{K_A}\right) \qquad \text{Equation 3}$$

$$D_c\left(\frac{\partial c_i}{\partial r}\right)_{r=R} = k_f(c - c_i) \qquad \text{Equation 4}$$

c = concentration of the compound in the inter-particle volume

c_i = concentration of the compound in the pore space

c_{ads} = concentration of adsorbed compound per unit mass of adsorbent

z = position along the bed

t = time

r = radial position in a particle

R = particle radius

E_a = effective axial dispersion coefficient

α = inter-particle void fraction

β = intra-particle void fraction

v = gas velocity

D_c = effective intra-particle diffusion coefficient

ρ_p = bulk density of the adsorbent

k_{ads} = adsorption rate constant

K_A = adsorption equilibrium constant

k_f = mass transfer coefficient

Equation 1 gives the material balance of the compound in the vapor phase [18]. Equation 2 gives the material balance of the compound in the particle [18]. Equation 3 gives the rate of adsorption onto the adsorptive sites within the adsorbent [18]. Equation 4 gives the external diffusion boundary condition [18]. When the external diffusion boundary condition is applied to equation 1, equation 5 is produced.

$$\frac{E_a}{\alpha}\frac{\partial^2 c}{\partial z^2} - \mathrm{v}\frac{\partial c}{\partial z} - \frac{\partial \mathrm{c}}{\partial \mathrm{t}} - \frac{3}{R}\frac{1-\alpha}{\alpha}k_f(c - c_i) = 0 \qquad \text{Equation 5}$$

Equation 5 represents the material balance in the gas phase but uses the mass transfer driving force to compute the loss of concentration from the inter-particle volume to the pore space. A similar form of this equation is used in many adsorption, chromatography, and filtration models[19-21]. Equations 5, 2, and 3 give a three equation system of differential equations that can be used to model the adsorptive bed system.

3.1.4 Graphical Representations of Adsorption Behavior

There are two major ways adsorption behavior can be graphically presented: as a peak in a chromatogram or as a breakthrough curve. A peak can be seen in the figure below. It is created by a single pulse of the compound and gives the concentration with

respect to time at the bed outlet. Peaks are useful as they are the output of a gas chromatograph and were the form from which all the experimental data in this thesis was gathered.

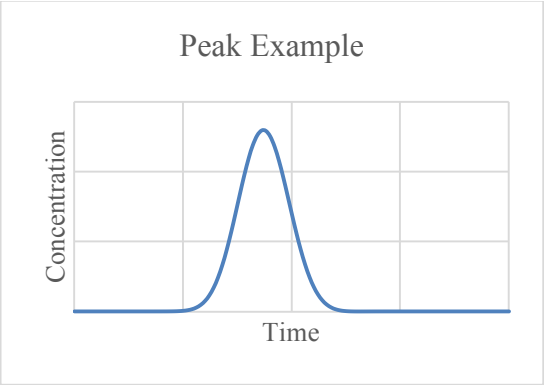

Figure 26. Example of a peak

A breakthrough curve can be seen in the figure below. A breakthrough curve is created from a steady and continuous flow of the compound through the bed. It represents the outlet concentration of a compound (sometimes as a ratio of the input concentration) with respect to time after the flow began. Breakthrough curves are useful as they present the real outlet and would be used to model a scaled up system. In other words, a peak would be the result of plotting the derivative of a breakthrough curve. The concentration ratio gives the ratio of the output concentration of a compound over the input concentration of that compound; this is a useful dimensionless variable to use when comparing and analyzing breakthrough curves.

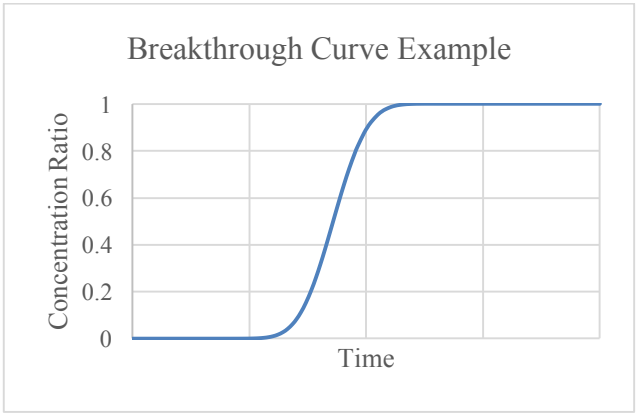

Figure 27. Example of a breakthrough curve using ratio of outlet concentration to inlet concentration as dependent variable

3.2 Numerically Modeling the PDEs Present in the Model

3.2.1 Software Considerations

The model given above uses partial differential equations (PDEs) in a system to model the adsorption process. In order to model this system of equations 5, 2, and 3, a direct numerical solution not requiring simplifying assumptions is preferred; however, partial differential equations are particularly difficult for software to solve given the multiple independent variables in the equation. Some software suites such as Matlab can solve some forms of PDEs found in engineering problems but these are generally a few very specific forms with respect to two position variables and no time variable. This particular system requires a different approach [20].

3.2.2 Discretization of PDEs

In order to solve this system of equations, equations 5 and 2 were converted to ordinary differential equations (ODEs) with time as the differential independent variable. The equations must be discretized with respect to the length coordinate – bed position (z) and particle radius (r) for equations 5 and 2 respectively. The

straightforward method of doing this is to apply finite differences to the length coordinates[20, 22]. Thus equation 5 becomes equation 6 and equation 2 becomes equation 7.

$$\frac{dc}{dt} = \frac{E_a}{\alpha}\frac{c(z+\Delta z) - c(z)^2 + c(z-\Delta z)}{\Delta z^2} - \mathrm{v}\frac{c(z+\Delta z) - c(z-\Delta z)}{2\Delta z} - \frac{3k_f(1-\alpha)\big(c(z) - c_i(z)\big)}{R\alpha} \qquad \text{Equation 6}$$

$$\frac{dc_i}{dt} = \frac{D_c}{\beta}\left(\frac{c_i(r+\Delta r) - c_i(r)^2 + c_i(r-\Delta r)}{\Delta r^2} + \frac{2}{r}\frac{c_i(r+\Delta r) - c_i(r-\Delta r)}{2\Delta r}\right) - \frac{\rho_p}{\beta}\frac{dc_{ads}}{dt} \qquad \text{Equation 7}$$

A step size is chosen for the z and r coordinates. For every axial position element in the bed Δz, there is an ODE in the form of equation 6 giving the concentration in the inter-particle space with respect to time in that element. For every radial element within an axial element Δr, there is an ODE in the form of equation 7 giving the concentration in the pore space with respect to time. This leads to the rapid increase in the number of ODEs in this system of equations. For example, if a model uses 50 axial elements and 10 radial elements, the model would be solving 550 simultaneous equations not considering the rate law given by equation 3. This can rapidly become a computationally intensive calculation.

3.2.3 Preliminary Assumptions

To simplify the calculation, certain simplifying assumptions were made. Axial dispersion is taken to be zero. This is a reasonable assumption given the high carrier gas velocity being used experimentally and is used in the literature [18]. Convection dominates rather than axial dispersion in causing transport of a compound through the

bed. Also, a diffusion effectiveness factor of 1 is used. Given the strong adsorption of phenolic compounds on activated carbon as well as the high gas velocity through the column, it seems reasonable to make this simplifying assumption.

3.3 Computational Challenges and Lessons

3.3.1 Execution Time

Unfortunately, even after the simplifying assumptions documented above were made, the computational resources proved insufficient to solve for a bed 27cm long which prevented a direct comparison to the experimental data. This is likely due to a step size issue. The software used to solve this system did not allow for the adjustment of the step size of the independent differential variable (time). The axial position step size can be adjusted by increasing the number of simultaneous ODEs, but a further increase in the number of steps (and decrease in step size) uses more system resources to finish the solution. The model both needs a larger step size to finish solving the entire time range and a smaller step size to prevent overshoot, undershoot, and coarse concentration profiles. This challenge prevented the program from successfully solving the system. Nonetheless, the model did work well at bed lengths around 1 cm and a sensitivity analysis of important variables can be conducted based on the reduced bed length.

3.3.2 Lessons from Modeling

Two useful parameters to determine are the adsorption equilibrium and adsorption rate constant. Ideally the model could be fit to the experimental data by adjusting these parameters. Adsorption rate and equilibrium constants would be the same for a small or large system as they depend on adsorbent and bed conditions but not

scale allowing for a model of a larger system to be produced. Even though this was ultimately not successful, an understanding of the effect of a change in one of these parameters is useful and can be generated from using a shorter bed length in the model. The figures below were generated using an external porosity of 0.5, a bulk density of 0.7 g/mL, and a bed length of 1 cm with 50 axial elements (steps).

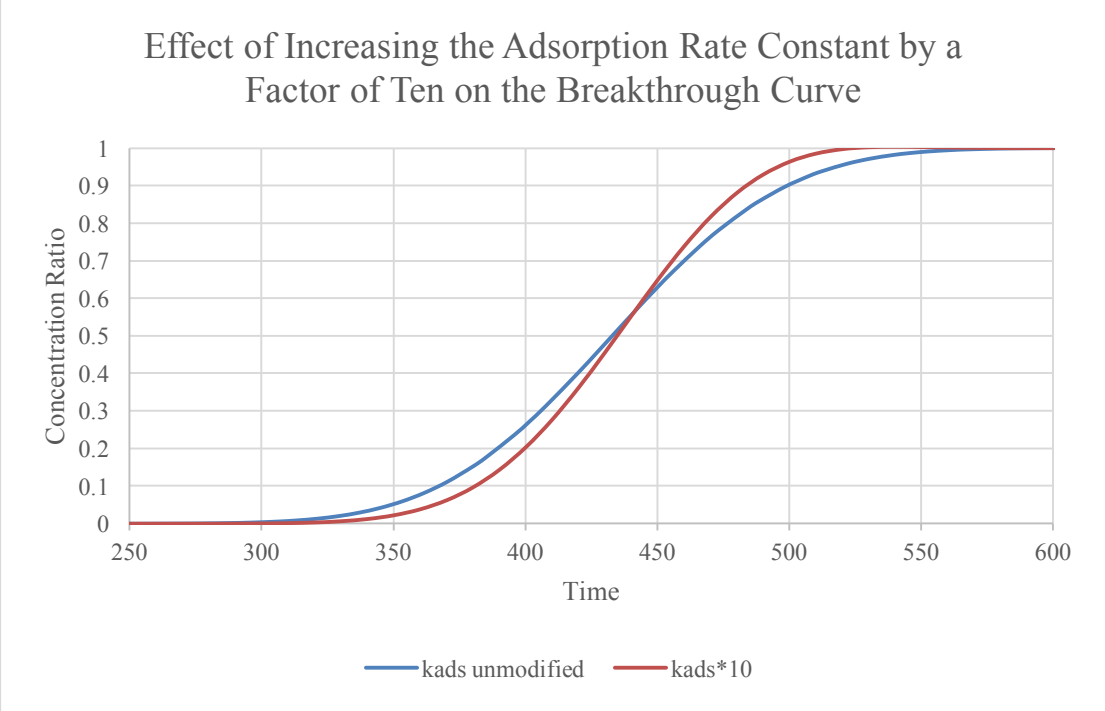

Figure 28. Effect of increasing the adsorption rate constant by a factor of ten on the breakthrough curve

In the figure above, the two curves appear to be superimposed; in fact, the point of inflection is nearly the same. It appears that the adsorption rate constant does not shift the breakthrough curve but instead sharpens it. The bed outlet for the model using the higher rate constant has a later breakthrough, but reaches maximum concentration sooner. The figure below illustrates the effects of doubling the adsorption equilibrium constant.

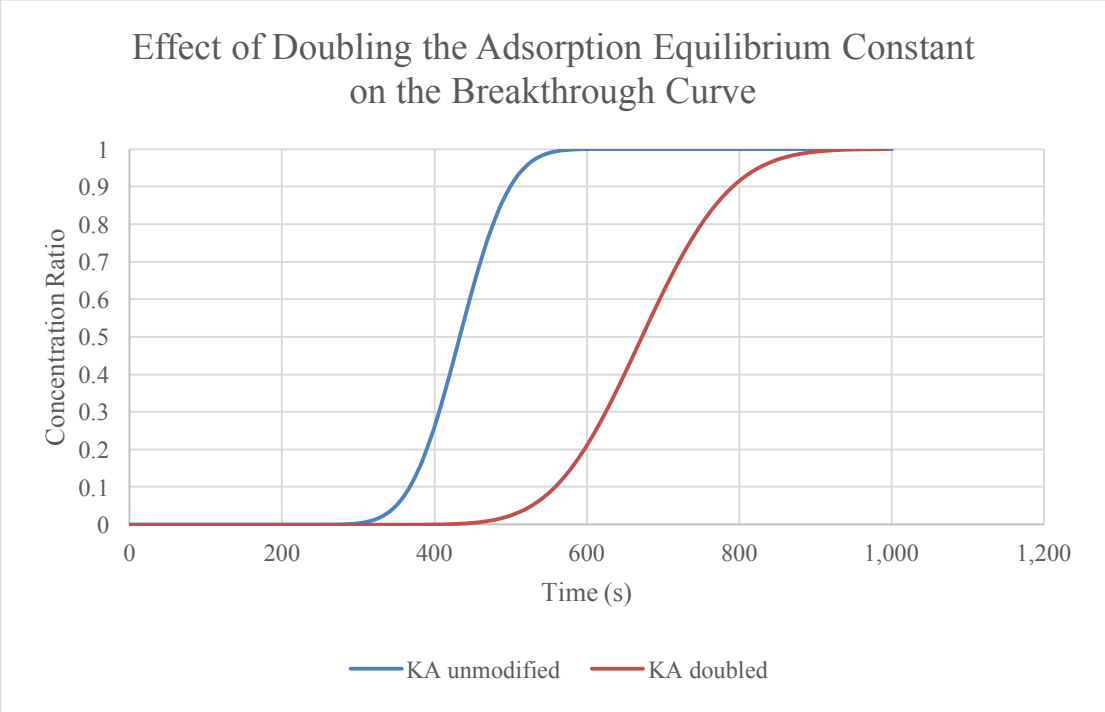

Figure 29. Effect of doubling the adsorption equilibrium constant on the breakthrough curve

Doubling the adsorption equilibrium constant has a rather different effect than increasing the adsorption rate constant. The breakthrough curve displaying the results of the model using the larger adsorption equilibrium constant occurs at a later time. While the increase does not appear to be directly proportional to the increase in equilibrium constant, there is a significant increase in time for the compound to first reach the end of the column. Also, the curve exhibits more spreading inasmuch as the point where breakthrough occurs is farther from the point of inflection.

A change in the adsorption equilibrium constant shifts the breakthrough curve due to shifting the adsorption/desorption equilibrium, while a change in the adsorption rate constant merely affects how rapidly that equilibrium is reached. Thus, a model

used to design a scaled up system will be more sensitive to an incorrect equilibrium constant.

Considering this modeling work overall, the equations themselves do seem to have the potential to effectively represent the physical adsorption system. Unfortunately, the software package used for these calculations was insufficiently robust given a smaller step size was needed to solve the model but unable to be used with the software. In the future, a more robust software package and perhaps supercomputer time should allow for both a finer step size creating a more accurate model as well as the many iterative solutions needed to be calculated when fitting experimental data to the model.

Chapter 4: Recommendations and Conclusion

4.1 Future Work

While there are many interesting possible paths on which to continue this research, a few stand out. First, it would be useful to confirm there are no reactions occurring on the surface of the activated carbon such as esterification. This could be done using a similar set up with a mass spectrometer. If a reaction is occurring within the column, the output streams will have different compositions that could either make future upgrading easier or more challenging.

A different apparatus might also be useful to conduct these adsorption experiments. The current apparatus only allows for pulse injections of a compound while a scaled up model would involve a step change in feed concentration. It would be useful to be able to experiment with step changes in feed on a small scale. This setup would have the advantage of having a more useful data output: the concentration profile would result in a breakthrough curve rather than a peak. Additionally, data outputted in a breakthrough curve might be easier to use to design a larger bed given it is already in the same form as is needed for the scale up process. There would be no need for a general adsorption model that can model both pulses resulting in peaks and step changes resulting in breakthrough curves. If the activated carbon is being permanently passivated to some extent, this apparatus would take that into account as there would be a larger number of moles of phenolic compounds flowing through it early in its life.

Two other avenues for future experimental work were already mentioned but worth revisiting. The retention time of the stage 1 liquid phenolic peak is earlier than is predicted by the model compound. Determining why this is the case would be useful as

this would affect the scalability modeling work as it would not be accurate to simply model the behavior of m-cresol. Also, determining the mechanism of passivation of the activated carbon might be useful as well. If the carbon can easily be reactivated by a steam or carbon dioxide flow, the needed bed sizes would be reduced.

In addition to using a more robust software package, it would be better to model the adsorbent bed using adsorbent weight as the independent axial variable rather than length. Given that the concentration should vary more repeatably with weight than length when using a different cross sectional area of the bed, this should allow for a better scale up. However, this may not be moot as it may not be possible or convenient with this model.

4.2 Conclusion of Experiments and Modeling

There are a few conclusions that can be drawn from this work. Acetic acid and phenolic compounds can be separated be the strength of their adsorption on activated carbon. Given the complexity of the stage 1 mixture, the degree of separation of the stage 1 mixture is less than an acetic acid and m-cresol model compound mixture on a bed of the same length. The modeling approach used will model the physical behavior of the system; however, more computing power will ultimately be needed to solve this complex system of equations.

References

1. Mohan, D., J. Charles U. Pittman, and P.H. Steele, *Pyrolysis of Wood/Biomass for Bio-oil: A Critical Review.* Energy & Fuels, 2006. **20**(3): p. 848-889.

2. Bridgwater, A.V., D.Meier, and D.Radlein, *An overview of fast pyrolysis of biomass.* Organic Geochemistry, 1999. **30**: p. 1479-1493.

3. de Wild, P., *Biomass Pyrolysis for Chemicals*, in *Mathematics and Natural Sciences*. 2011, University of Groningen.

4. Waters, C.L., *Understanding Thermochemical Process and Feedstock Compositional Impacts on Strategies to Control Pyrolysis and Torrefaction Product Distributions*, in *School of Chemical, Biological and Materials Engineering*. 2016, University of Oklahoma: Norman, Oklahoma.

5. Kersten, S.R.A., et al., *Biomass pyrolysis in a fluidized bed reactor. Part 1: Literature review and model simulations.* Industrial & Engineering Chemistry Research, 2005. **44**(23): p. 8773-8785.

6. Zaimes, G.G., et al., *Multistage torrefaction and in situ catalytic upgrading to hydrocarbon biofuels: analysis of life cycle energy use and greenhouse gas emissions.* Energy & Environmental Science, 2017. **10**(5): p. 1034-1050.

7. Resasco, D.E. and S.P. Crossley, *Implementation of concepts derived from model compound studies in the separation and conversion of bio-oil to fuel.* Catalysis Today, 2015. **257**: p. 185-199.

8. Pham, T.N., D.C. Shi, and D.E. Resasco, *Evaluating strategies for catalytic upgrading of pyrolysis oil in liquid phase.* Applied Catalysis B-Environmental, 2014. **145**: p. 10-23.

9. Rezaei, P.S., H. Shafaghat, and W.M.A.W. Daud, *Aromatic hydrocarbon production by catalytic pyrolysis of palm kernel shell waste using a bifunctional Fe/HBeta catalyst: effect of lignin-derived phenolics on zeolite deactivation.* Green Chemistry, 2016. **18**(6): p. 1684-1693.

10. Du, S., J.A. Valla, and G.M. Bollas, *Characteristics and origin of char and coke from fast and slow, catalytic and thermal pyrolysis of biomass and relevant model compounds.* Green Chemistry, 2013. **15**: p. 3214-3229.

11. Fogler, H.S., *Elements of Chemical Reaction Engineering*. Fourth ed. 2006, Westford, Massachusetts: Pearson Education.

12. Dabrowski, A., et al., *Adsorption of phenolic compounds by activated carbon--a critical review.* Chemosphere, 2005. **58**(8): p. 1049-70.

13. Harris, P.J.F., Z. Liu, and K. Suenaga, *Imaging the atomic structure of activated carbon.* Journal of Physics: Condensed Matter, 2008. **20**(36).

14. Bansal, R.C. and M. Goyal, *Activated Carbon Adsorption*. 2005, Boca Raton, FL: CRC Press.

15. Figueiredo, J.L., et al., *Modification of the surface chemistry of activated carbons.* Carbon, 1999. **37**: p. 1379-1389.

16. Elhussien, M.H. and Y.M. Isa, *Acetic Acid Adsorption onto Activated Carbon Derived from Pods of Acacia nilotica var astringens (Sunt tree) by Chemical Activation with $ZnCl_2$.* Journal of Natural Sciences Research, 2015. **5**(10): p. 42-48.

17. Olsen, T., *An Oil Refinery Walk-Through*, in *Chemical Engineering Progress*. 2014, AIChE. p. 34-40.

18. Schneider, P. and J.M. Smith, *Adsorption Rate Constants from Chromatography.* AIChE Journal, 1968. **14**(5): p. 762-771.

19. Harrison, R.G., et al., *Bioseparations Science and Engineering*. Second ed. 2015, New York, NY: Oxford University Press.

20. Pham, N.H., et al., *Transport and deposition kinetics of polymer-coated multiwalled carbon nanotubes in packed beds.* AIChE Journal, 2016. **62**(10): p. 3774-3783.

21. Qamar, S., N. Akram, and A. Seidel-Morgenstern, *Analysis of general rate model of linear chromatography considering finite rates of the adsorption and desorption steps.* Chemical Engineering Research and Design, 2016. **111**: p. 13-23.

22. Chapra, S.C. and R.P. Canale, *Numerical Methods for Engineers*. Seventh ed. 2015, New York, NY: McGraw Hill.